A rate- and state-dependent ductile flow law of polycrystalline halite under large shear strain and implications for transition to brittle deformation

Hiroyuki Noda[1] and Toshihiko Shimamoto[2,3]

Received 13 January 2010; revised 25 March 2010; accepted 5 April 2010; published 15 May 2010.

[1] We have conducted double-shear biaxial deformation experiments in layers of NaCl within its fully-plastic (FP) regime up to large shear strains ($\gamma < 50$) with velocity steps. From this, we have empirically formulated a rate- and state-dependent flow law which explains the transient mechanical behavior. The steady state flow stress in the FP regime can be explained by a power-law with a stress exponent ~8.5 and an activation enthalpy of ~1.3 eV, with the instantaneous response having a higher stress exponent (13 ± 8), although there is data scatter. The transition to brittle regime is associated with weakening from the ductile flow law. In FP regime, the mechanical response is characterized by a monotonic decay to a new steady state while in the transitional regime, by a peak-decay behavior. The transient flow law obtained here is of considerable importance in the study of the brittle-ductile transition in rocks. **Citation:** Noda, H., and T. Shimamoto (2010), A rate- and state-dependent ductile flow law of polycrystalline halite under large shear strain and implications for transition to brittle deformation, *Geophys. Res. Lett.*, *37*, L09310, doi:10.1029/2010GL042512.

1. Introduction

[2] Halite (NaCl) is one of the rock-forming minerals which undergoes a brittle-ductile transition under experimentally convenient conditions, and thus is often used as an analogue material to investigate rock deformation mechanisms near the down-dip limit of the seismogenic zone [e.g., *Shimamoto*, 1986; *Kawamoto and Shimamoto*, 1997; *Niemeijer and Spiers*, 2006]. In addition, it has importance in related fields such as engineering and environment; halite forms salt domes which can potentially act as a cap rock for petroleum and natural or injected gas, as well as the storage of nuclear waste. The formulation of a ductile flow law for NaCl which includes the transient behavior is important if such problems are to be realistically considered. It provides fundamental information on the brittle-ductile transition by giving one of the end members. In spite of these significances, such a law has been poorly investigated, especially at large shear strains which are relevant to natural conditions. Previous studies on the deformation mechanism of NaCl under its fully-plastic condition [e.g., *Verrall et al.*, 1977; *Frost and Ashby*, 1982] are based on a series of compression, tensile, bending, and hardness tests in which large shear strains and transient changes in the strain rate are difficult to apply. In order to study the constitutive law at a large strain, other methods are required. Note that in this paper, the "fully-plastic" (FP) condition or regime is defined as a condition or a range of conditions where the flow stress of the material has little dependence on the mean stress or normal stress, following the definition by *Kawamoto and Shimamoto* [1997].

[3] In this study, we have conducted double-shear biaxial deformation experiments (inset in Figure 1a) with steps in the load point velocity (LPV), and conducted iterative least-squares fitting [*Reinen and Weeks*, 1993; *Noda and Shimamoto*, 2009] in order to determine the constitutive parameters appearing in an assumed transient flow law. This method has been developed for decades for the purpose of investigating frictional constitutive laws in which the flow stress is approximately proportional to the normal stress. However, the application of this method to the ductile shear zone is new and turns out to be very significant as shown in the following section.

2. Methodology

[4] We conducted a series of experiments on layers of polycrystalline NaCl using a high-temperature biaxial deformation apparatus at Hiroshima University [*Kawamoto and Shimamoto*, 1997, 1998]. These layers were sandwiched between host rocks consisting of gabbro brocks, with a NaCl layer thickness of ~0.4 mm, 5 cm long in the shear direction and 4 cm wide. The combination of such thin shear zones and the ability to produce long slip displacements (~20 mm) enables us to produce a very large shear strain (γ = macroscopic slip/shear zone width) up to 50, which is the significant advantage of this experimental configuration. The faces of host rocks in contact with the NaCl layers were polished using #60 carborundom. We put 1.5 g of NaCl powder (<100 μm in diameter) on the side blocks, assembled the blocks, and pre-compacted the layers at the given experimental conditions for about 1 hour before applying shear deformation.

[5] First, we retested the brittle-ductile transition observed by *Kawamoto and Shimamoto* [1997] by changing the normal stress and the temperature in steps, using crushed rock salt (Sicily) and synthetic NaCl. Then, we focused on the transient behavior in the FP regime for synthetic NaCl by conducting a series of velocity step tests (abrupt changes in LPV). These were conducted at temperatures ranging from 185–500°C, and at a shear strain rate ($\dot{\gamma}$ = macroscopic

[1]Seismological Laboratory, California Institute of Technology, Pasadena, California, USA.
[2]Graduate School of Sciences, Hiroshima University, Higashi-Hiroshima, Japan.
[3]Now at Institute of Geology, China Earthquake Administration, Beijing, China.

0094-8276/10/2010GL042512

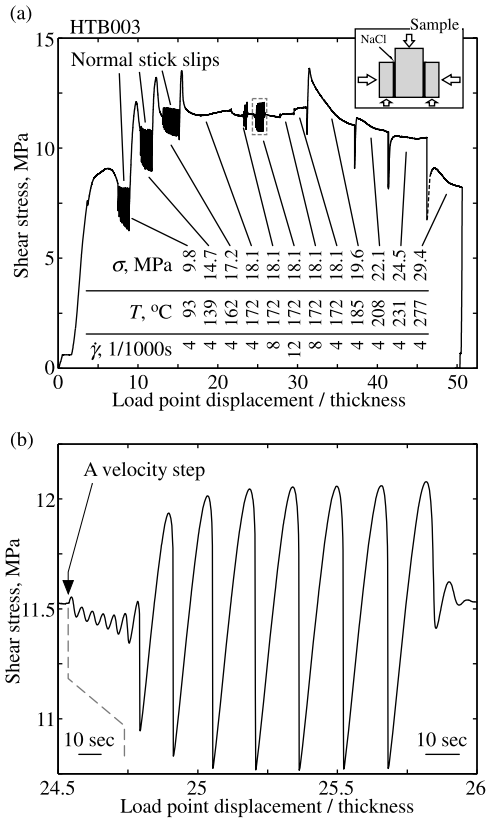

Figure 1. (a) Experimental results for crushed rock-salt crossing the brittle-ductile transition by varying temperature and normal stress. The inset shows the specimen assembly. (b) A magnified plot of Figure 1a (indicated by dashed square) showing slow stick-slips near the brittle-ductile transition. Scales for time are indicated for before and after a velocity step.

slip rate/shear zone width) on the order of 10^{-3}–10^{-1}/s every 1.5 mm of the load point displacement (about 3.75 in γ). We applied a normal stress of 39.2 MPa to prevent brittle deformation.

[6] The mechanical data for each of the velocity steps are used to determine the parameters appearing in the constitutive law which is described in the following section by conducting iterative least-squares fitting [*Reinen and Weeks*, 1993; *Noda and Shimamoto*, 2009]. For detailed numerical methodology, see *Noda and Shimamoto* [2009].

3. Results and Discussion

3.1. Overall Behavior When Crossing the Brittle-Ductile Transition

[7] Figure 1a shows the overall behavior when crossing the brittle-ductile transition for crushed rock salt. At low temperatures and low normal stresses, we observed an increase in the shear stress with increasing normal stress, which is a characteristic of brittle behavior. Also, we obtained stick-slip events, indicating that the friction is rate-weakening. Note that if stick-slip events occur, it is difficult to further investigate the constitutive law accounting for a transient behavior. Also note that the horizontal axis in Figure 1 represents the load point displacement (sum of slip displacement of the shear zone and deformation of spacers and host rocks) from the start of the experiments divided by the shear zone thickness, and not the actual plastic shear strain of the shear zone.

[8] At 18.1 MPa and 172°C, the rapid stick-slip events disappear. Within this transitional regime we occasionally observe an oscillatory behavior or slow stick-slip events (Figure 1b). We would like to emphasise that it is hasty to directly compare this behavior to naturally observed slow slip events or slow earthquakes near the down-dip limit of large earthquakes [e.g., *Obara*, 2002; *Hirose and Obara*, 2005; *Ide et al.*, 2007]. In the lab-frictional experiments, the transition between stable and unstable sliding depends on the machine stiffness in addition to the frictional constitutive law, and it has long been understood that the sliding behavior becomes oscillatory near the transition between stable sliding and stick-slip [*Ruina*, 1983; *Rice and Ruina*, 1983; *Gu et al.*, 1984]. In order to understand the slow events, we have to consider the coupling of a fault constitutive law and a surrounding medium [e.g., *Liu and Rice*, 2005].

[9] As the temperature increases further, the flow stress decreases even with increasing normal stress. This is a characteristic within the FP regime where the effect of temperature becomes more important than that of the normal stress [*Kawamoto and Shimamoto*, 1997].

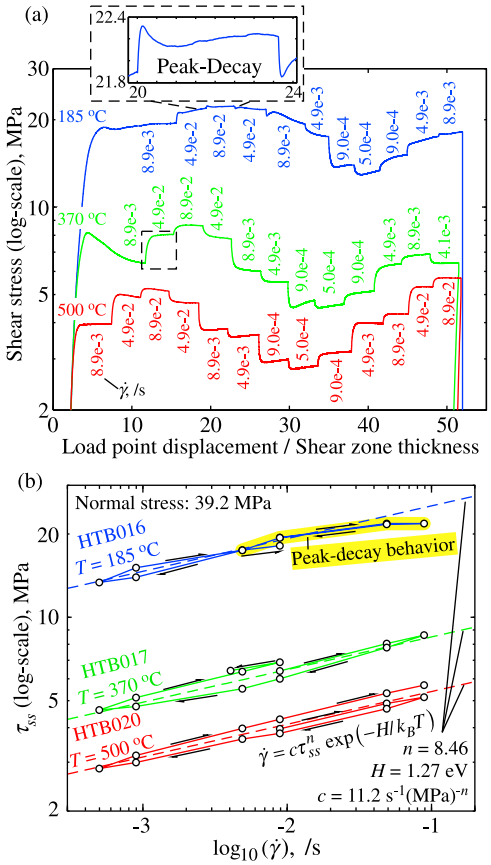

Figure 2. (a) Mechanical behavior observed for a series for velocity step tests at different temperatures (185°C, 370°C, and 500°C). σ = 39.2 MPa. (b) Steady-state shear stress as a function of strain rate at different temperatures.

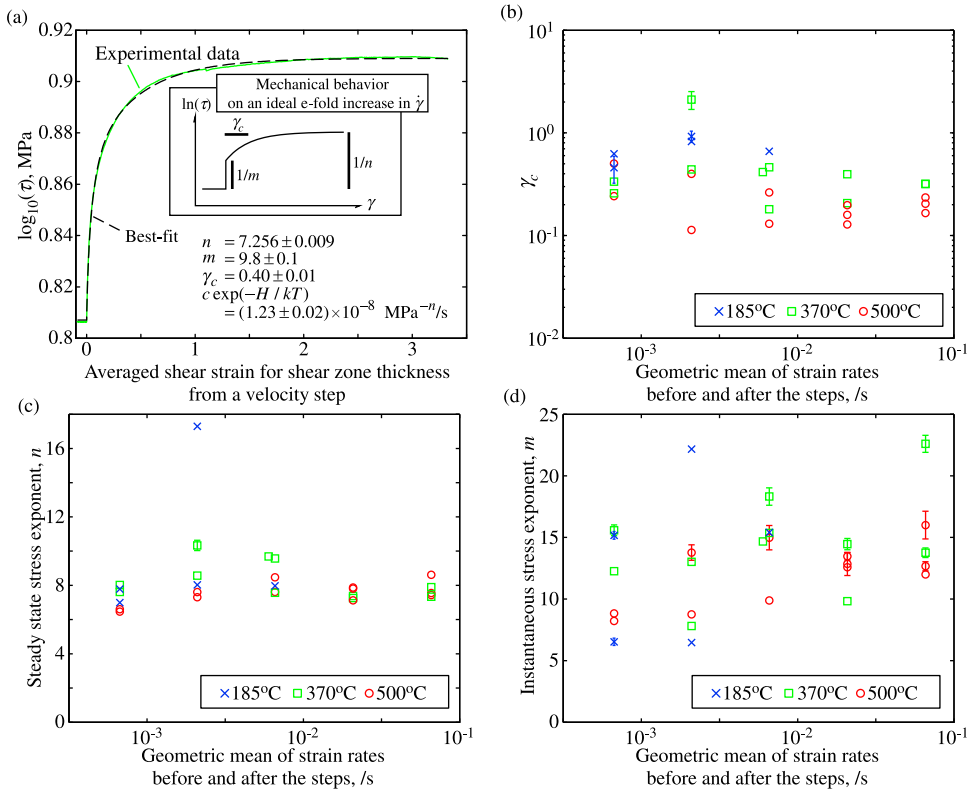

Figure 3. Results of least-squares fitting of a rate- and state-dependent flow law (equations (2)–(4)). Crosses: 185°C, squares: 370°C, circles: 500°C. (a) An example of fitting to a velocity step test indicated by dashed square in Figure 2a. (b) Characteristic shear strain for the state evolution, γ_c. (c) Stress exponent for the steady state, n. (d) Stress exponent for the instantaneous effect, m.

3.2. Ductile Flow Law With Transient Behavior

[10] Figure 2a shows a series of velocity step tests conducted mainly within the FP regime. Most of the (positive/negative) velocity steps are followed by monotonic (positive/negative) decays in the flow stress towards its new steady state value, τ_{ss}, with a minor contribution from the long-wavelength perturbation. Exceptions to this are seen at low temperature (185°C) and high strain rates which show a peak-decay behavior (inset in Figure 2a). These cases are affected by the frictional constitutive law which predicts such a behavior for an abrupt jump in the slip rate [*Dieterich*, 1979]. τ_{ss} defined just before the velocity steps are plotted in Figure 2b. τ_{ss} diverges from a power law at this transitional regime.

[11] For the steady state flow stress in the FP regime, we have adopted

$$\dot{\gamma} = c\tau_{ss}{}^{n} \exp(-H/k_B T). \tag{1}$$

where n is a stress exponent at a steady state, c is a constant, H is the activation enthalpy, k_B is the Boltzmann constant, and T is the absolute temperature. Our experimental data is explained by equation (1) with n and H about 8.5 and 1.3 eV, respectively. These values are consistent with previous studies conducted under similar conditions by *Kawamoto and Shimamoto* [1997]. Though the very high stress exponent may represent the experimental condition is nearing a power law breakdown, we use the power law for the purpose of empirical fit to the mechanical data. Note that the shear strain used in this work is much larger than what is typically used to investigate the flow law of crystalline materials.

[12] We formulate a rate- and state-dependent flow law as

$$d\ln(\tau/\tau_r) = \frac{n}{m} d\ln(\tau_{ss}/\tau_r) + d\Psi. \tag{2}$$

where m is a power exponent in an instantaneous response τ_r is an arbitrary reference shear stress (e.g. 1 MPa), and Ψ is a state variable which evolves by

$$d\Psi = (d\gamma/\gamma_c) \cdot \ln(\tau_{ss}/\tau) \tag{3}$$

where γ_c is the characteristic shear strain of the state evolution. On an ideal increase in $\dot{\gamma}$ by a factor of e, τ instantaneously increases by a factor of $\exp(1/m)$ followed by an asymptotic change by a factor of $\exp(1/n - 1/m)$ (inset in Figure 3a). $n \le m$ and $n > m$ yield monotonic and peak-decay behaviors, respectively. Previous studies by *Mitra and McLean* [1967] and *Hart* [1970] considered both rate- and state-dependency to deal with work hardening. *Pontikis and Poirier* [1975] conducted creep tests with jumps in the load, and demonstrated a peak-decay behaviour in the strain rate which is predicted for the case of $n < m$.

[13] As τ changes, the apparatus itself will inevitably deform elastically by

$$d\tau = k_s(dD - d\delta) = k_s(Udt - wd\gamma) \tag{4}$$

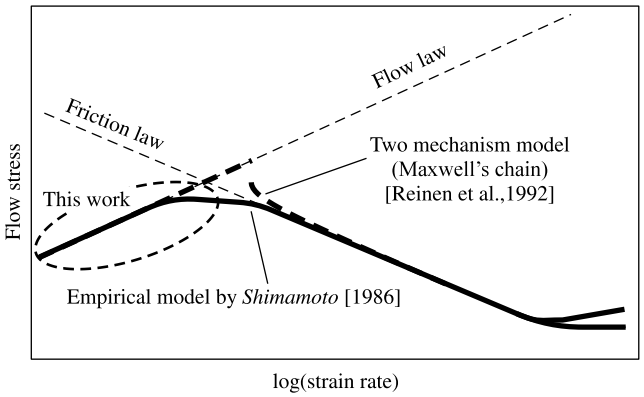

Figure 4. A schematic diagram showing the brittle-ductile transition as a function of the strain rate, modified from *Shimamoto* [1986]. An expected steady state behavior from model by *Reinen et al.* [1992] is shown by heavy dashed lines.

where k_s is the machine stiffness, D is the load point displacement which is determined by the rotation rate of the servo-motor and the gear ratio, δ is the slip in the shear layers, U is LPV, and w is the width of the shear zone assumed to be constant. It has been shown that the elastic deformation of the apparatus must be taken into consideration in order to accurately determine the parameters [*Reinen and Weeks*, 1993; *Noda and Shimamoto*, 2009].

[14] We have numerically integrated equations (2)–(4), and fit the solution by solving the least-squares problem iteratively to each velocity step after the removal of the overall trend. An initial steady state is assumed, and U is changed abruptly upon a velocity step.

[15] The advantage of such biaxial deformation test is the low noise level as shown in Figure 3a. The experimental configuration requires neither a jacket around the shear zone nor a pressure vessel unlike in triaxial sawcut tests, so there is no need to made a correction to the mechanical data to account for the strength of the jacket and O-rings. This method is suitable for the analysis of transient behaviors, the amplitude of which is much smaller than the absolute value of the flow stress. Note that we have also tested both purely direct ($\gamma_c = 0$) and purely indirect ($m = \infty$) laws. The former cannot explain the mechanical data well, and the latter is irrelevant; we have to allow an abrupt change in $\dot{\gamma}$ on a velocity step while τ changes continuously. Fitting of the purely indirect law requires about 3 order of magnitude larger optimum k_s than what is expected from a direct measurement of a spring constant [*Noda and Shimamoto*, 2009], and there is no resolution to invert for k_s with large relative error. In the case used in Figure 3a, an optimum value of k_s using a purely indirect law is 7×10^6 MPa/m with a relative error of 4700%, while the rate- and state-dependent law yielded $k_s = (1.65 \pm 0.02) \times 10^4$ MPa/m.

[16] Figures 3b–3d summarize constitutive parameters as a function of $\dot{\gamma}$. The velocity steps with peak-decay behavior (indicated in Figure 2b) are exempted. The error bars (2σ) obtained by each fitting is plotted only if it is visibly long. The data scatters more widely than these error bars, indicating that the overall error is determined by the repeatability of the velocity steps. Figure 3b indicates that γ_c is independent on $\dot{\gamma}$ for more than 2 orders of magnitude, indicating that the physical process governing the state evolution is controlled by shear strain rather than time. n (Figure 3c) is 7.9 ± 1.8 (2σ) with an exceptionally high value near the brittle-ductile transition. m ranges 13 ± 8 (2σ) which shows large scattering, with n/m being 0.61 ± 0.24 (2σ) omitting points larger than 1 (peak-decay behavior) which are affected by a long-wavelength fluctuation. We would like to emphasize that the method we took in this work is a new tool to investigate the transient flow law of a material in its FP regime with very large strain.

[17] One of the possible mechanisms for the state-dependency is the competition of work-hardening and its recovery. Further investigation including microstructural observation is required although the preservation of NaCl microstructures is challenging as they change very rapidly after an experiment [*Shimamoto and Logan*, 1986; *Hiraga and Shimamoto*, 1987].

3.3. Transitional Behavior to Brittle Deformation

[18] The transition to peak-decay behavior is associated with a decrease in the steady state flow stress from the extrapolation of the flow law in the FP regime (Figures 2b and 4). *Reinen et al.* [1992] connected the frictional (peak-decay) and what they call "flow" (monotonic decay) behaviors by Maxwell's chain of two constitutive laws (Figure 4) for serpentine minerals. *Chester and Higgs* [1992] also explains their experiments in quartz gouge using the same model. The decrease in the steady-state flow stress at the transition (Figure 2b) opposes Reinen's model, and previous work on the texture of experimentally deformed NaCl [*Hiraga and Shimamoto*, 1987] revealed a complicated transition from one concentrated slip plane to multiple slip planes before distributed deformation throughout the sample, though the texture may depend on the rock type. Maxwell's chain is applicable if a frictional surface is developed inside a shear layer. Such a surface is characterized by much smaller real area of contact than the nominal area of the frictional surface while the ductile flow of crystalline material is typically considered neglecting the porosity. Therefore, the transition to brittle regime should correspond to the decrease in the contact area which is consistent with the decrease in flow stress. Also, frictional constitutive laws are usually based on an exponential law rather than a power law, indicating the change in the deformation mechanism between the bulk flow studied in this work and a highly concentrated deformation at contacts on a frictional surface. The actual formulation of the constitutive law in this transitional regime requires further work including theoretical studies and microstructural observations.

4. Summary

[19] We have conducted velocity step tests on shear layers of NaCl mainly under ductile conditions. The mechanical data for a velocity step shows a monotonic decay to a new steady state. By numerical fitting of assumed constitutive laws to the observed mechanical data, we found a formulation of the transient flow law which has both rate- and state-dependencies. The parameters appearing in our law shows little dependency on the experimental conditions (the temperature and the strain rate). We also observed the transition to the regime which is characterized by a peak-

decay behavior upon a velocity step. This transition is associated with a decrease in the steady state flow stress which is extrapolated from the FP regime, and cannot be explained by the two mechanism model proposed by *Reinen et al.* [1992]. The transient flow law describing this transitional regime requires further work.

[20] **Acknowledgments.** We gratefully appreciate the grammatical check by Tom Mitchell, and comments by Masao Nakatani which improved the manuscript.

References

Chester, F., and N. Higgs (1992), Multimechanism friction constitutive model for ultrafine quartz gouge at hypocentral conditions, *J. Geophys. Res.*, *97*, 1859–1870, doi:10.1029/91JB02349.

Dieterich, J. H. (1979), Modeling of rock friction: 1. Experimental results and constitutive equations, *J. Geophys. Res.*, *84*, 2161–2168, doi:10.1029/JB084iB05p02161.

Frost, H. J., and M. F. Ashby (1982), *Deformation-Mechanism Maps: The Plasticity and Creep of Metals and Ceramics*, 184 pp., Pergamon, Oxford, U. K.

Gu, J.-C., J. R. Rice, A. L. Ruina, and S. T. Tse (1984), Slip motion and stability of a single degree of freedom elastic system with rate and state dependent friction, *J. Mech. Phys. Solids*, *32*, 167–196, doi:10.1016/0022-5096(84)90007-3.

Hart, E. W. (1970), A phenomenological theory for plastic deformation of polycrystalline metals, *Acta Metall.*, *18*, 599–610, doi:10.1016/0001-6160(70)90089-1.

Hiraga, H., and T. Shimamoto (1987), Textures of sheared halite and their implications for the seismogenic slip of deep faults, *Tectonophysics*, *144*, 69–86, doi:10.1016/0040-1951(87)90009-6.

Hirose, H., and K. Obara (2005), Repeating short- and long-term slow slip events with deep tremor activity, around the Bungo channel region, southwest Japan, *Earth Planets Space*, *57*, 961–972.

Ide, S., G. C. Beroza, D. R. Shelly, and T. Uchide (2007), A scaling law for slow earthquakes, *Nature*, *447*, doi:10.1038/nature05780.

Kawamoto, E., and T. Shimamoto (1997), Mechanical behavior of halite and calcite shear zones from brittle to fully-plastic deformation and a revised fault model, in *Proceedings of the 30th International Geological Congress, Beijing, China, 4–14 August 1996*, vol. 14, pp. 89–105.3, VSP, Utrecht, Netherlands.

Kawamoto, E., and T. Shimamoto (1998), The strength profile for bimineralic shear zones: An insight from high-temperature shearing experiments on calcite-halite mixtures, *Tectonophysics*, *295*, 1–14, doi:10.1016/S0040-1951(98)00112-7.

Liu, Y., and J. R. Rice (2005), Aseismic slip transients emerge spontaneously in three-dimensional rate and state modeling of subduction earthquake sequences, *J. Geophys. Res.*, *110*, B08307, doi:10.1029/2004JB003424.

Mitra, S. K., and D. McLean (1967), Cold work and recovery in creep at ostensibly constant structure, *Metal Sci. J.*, *1*, 192–198.

Niemeijer, A. R., and C. J. Spiers (2006), Velocity dependence of strength and healing behavior in simulated phyllosilicate-bearing fault gouge, in *Deformation Mechanisms, Rheology and Tectonics Conference*, edited by N. S. Mancktelow and L. Burlini, pp. 231–253, Elsevier, Amsterdam.

Noda, H., and T. Shimamoto (2009), Constitutive properties of clayey fault gouge from Hanaore fault zone, southwest Japan, *J. Geophys. Res.*, *114*, B04409, doi:10.1029/2008JB005683.

Obara, K. (2002), Nonvolcanic deep tremor associated with subduction in southwest Japan, *Science*, *296*, 1679–1681, doi:10.1126/science.1070378.

Pontikis, V., and J. P. Poirier (1975), Phenomenological and structural analysis of recovery-controlled creep, with special reference to the creep of single crystal silver chloride, *Philos. Mag.*, *32*, 577–592, doi:10.1080/14786437508220881.

Reinen, L. A., and J. D. Weeks (1993), Determination of rock friction constitutive parameters using an iterative least square inversion method, *J. Geophys. Res.*, *98*, 15,937–15,950, doi:10.1029/93JB00780.

Reinen, L. A., T. E. Tullis, and J. D. Weeks (1992), Two-mechanism model for frictional sliding of serpentinite, *Geophys. Res. Lett.*, *19*(15), 1535–1538, doi:10.1029/92GL01388.

Rice, J. R., and A. L. Ruina (1983), Stability of steady frictional slipping, *J. Appl. Mech.*, *50*, 343–349, doi:10.1115/1.3167042.

Ruina, A. L. (1983), Slip instability and state variable friction laws, *J. Geophys. Res.*, *88*, 10,359–10,370, doi:10.1029/JB088iB12p10359.

Shimamoto, T. (1986), Transition between frictional slip and ductile flow for halite shear zones at room temperature, *Science*, *231*, 711–714, doi:10.1126/science.231.4739.711.

Shimamoto, T., and J. W. Logan (1986), Velocity-dependent behaviors of simulated halite shear zones: An analog for silicates, in *Earthquake Source Mechanics*, *Geophys. Monogr. Ser.*, vol. 37, edited by S. Das et al., pp. 49–63, AGU, Washington, D. C.

Verrall, R. A., R. J. Fields, and M. F. Ashby (1977), Deformation-mechanism maps for. LiF and NaC1, *J. Am. Ceram. Soc.*, *60*, 211–216, doi:10.1111/j.1151-2916.1977.tb14108.x.

H. Noda, Seismological Laboratory, California Institute of Technology, 1200 E. California Blvd., Pasadena, CA 91125, USA. (hnoda@caltech.edu)

T. Shimamoto, Institute of Geology, China Earthquake Administration, PO Box 9803, Beijing 100029, China.